Experimental Gerontology 178 (2023) 112201

Contents lists available at ScienceDirect

Experimental Gerontology

journal homepage: www.elsevier.com/locate/expgero

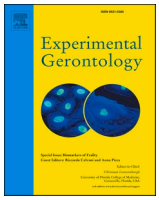

Diclofenac, a NSAID, delays fracture healing in aged mice

Maximilian M. Menger [a,b,*], Maximilian Stief [b], Claudia Scheuer [b], Mika F. Rollmann [a], Steven C. Herath [a], Benedikt J. Braun [a], Sabrina Ehnert [a,c], Andreas K. Nussler [a,c], Michael D. Menger [b], Matthias W. Laschke [b], Tina Histing [a]

[a] Department of Trauma and Reconstructive Surgery, Eberhard Karls University Tuebingen, BG Trauma Center Tuebingen, 72076 Tuebingen, Germany
[b] Institute for Clinical & Experimental Surgery, Saarland University, 66421 Homburg, Saar, Germany
[c] Department of Trauma and Reconstructive Surgery, BG Trauma Center Tuebingen, Siegfried Weller Institute for Trauma Research, Eberhard Karls University Tuebingen, 72076 Tuebingen, Germany

ARTICLE INFO

Section Editor: Christiaan Leeuwenburgh

Keywords:
Diclofenac
Bone healing
Fracture repair
Bone remodeling
Age
Osteoclast activity
Angiogenic growth factors
Osteogenic growth factors
RANKL
OPG

ABSTRACT

Nonsteroidal anti-inflammatory drugs (NSAIDs), such as diclofenac, belong to the most prescribed analgesic medication after traumatic injuries. However, there is accumulating evidence that NSAIDs impair fracture healing. Because bone regeneration in aged patients is subject to significant changes in cell differentiation and proliferation as well as a markedly altered pharmacological action of drugs, we herein analyzed the effects of diclofenac on bone healing in aged mice using a stable closed femoral facture model. Thirty-three mice (male $n = 14$, female $n = 19$) received a daily intraperitoneal injection of diclofenac (5 mg/kg body weight). Vehicle-treated mice ($n = 29$; male $n = 13$, female $n = 16$) served as controls. Fractured mice femora were analyzed by means of X-ray, biomechanics, micro computed tomography (μCT), histology and Western blotting. Biomechanical analyses revealed a significantly reduced bending stiffness in diclofenac-treated animals at 5 weeks after fracture when compared to vehicle-treated controls. Moreover, the callus tissue in diclofenac-treated aged animals exhibited a significantly reduced amount of bone tissue and higher amounts of fibrous tissue. Further histological analyses demonstrated less lamellar bone after diclofenac treatment, indicating a delay in callus remodeling. This was associated with a decreased number of osteoclasts and an increased expression of osteoprotegerin (OPG) during the early phase of fracture healing. These findings indicate that diclofenac delays fracture healing in aged mice by affecting osteogenic growth factor expression and bone formation as well as osteoclast activity and callus remodeling.

1. Introduction

With a steadily increasing older population, the treatment of geriatric patients has become a major challenge in modern trauma and orthopedic surgery (Rollmann et al., 2019). Older adults do not only have a higher risk of fractures, but also suffer from an enhanced mortality and reduced bone healing potential. The resulting incapacitations of delayed healing and non-union formation are not only associated with additional pain and loss of function, but also delay the rehabilitation process and, thus, pose a substantial burden on the health care system (Rose and Maffulli, 1999; Cauley et al., 2000; Green et al., 2005).

Nonsteroidal anti-inflammatory drugs (NSAIDs), such as diclofenac, are frequently used in the treatment of orthopedic injuries due to their excellent antiphlogistic, antipyretic and analgesic properties (Dodwell et al., 2010). However, a variety of preclinical studies demonstrated detrimental effects of diclofenac on bone regeneration (Beck et al., 2003; Krischak et al., 2007). Potential underlying pathophysiological mechanisms may include the inhibition of cyclooxygenase (COX-2) and prostaglandins, which are both essential mediators during the inflammatory phase of fracture healing (Ramirez-Garcia-Luna et al., 2019), but also an impaired communication between osteoclasts and osteoblasts via the receptor activator of NF-κB ligand (RANKL) and osteoprotegerin (OPG) (Haversath et al., 2012).

In old individuals, however, there is a complete lack of information about the effects of diclofenac on bone healing and regeneration. In geriatric patients, fracture healing is subject to significant physiological

* Corresponding author at: Department of Trauma and Reconstructive Surgery, BG Trauma Center Tuebingen, Eberhard Karls University Tuebingen, 72076 Tuebingen, Germany.
E-mail address: maximilian.menger@uks.eu (M.M. Menger).

https://doi.org/10.1016/j.exger.2023.112201
Received 24 December 2022; Received in revised form 6 May 2023; Accepted 8 May 2023
Available online 23 May 2023

changes, including a decreased stem cell proliferation and a delay in chondro- and osteogenesis (Gruber et al., 2006; Lu et al., 2005). Furthermore, aging results in a progressive decline in the functional reserve of multiple organs, such as hepatic clearance and renal extraction. Hence, pharmacokinetics, metabolism and drug actions may be significantly altered in old adults when compared to the young (Klotz, 2009). Therefore, we herein analyzed for the first time the effects of diclofenac on bone healing and regeneration in aged mice using a well-established stable closed fracture model. The callus tissue of fractured mice femora was analyzed by radiological, biomechanical, histological and biochemical techniques at 2 and 5 weeks after fracture.

2. Material and methods

2.1. Animals

For the present study a total number of 62 male and female CD-1 mice with an age of 16–18 months were used. The animals were bred at the Institute for Clinical & Experimental Surgery, Saarland University, and kept at a regular light and dark cycle with free access to tap water and standard pellet food (Altromin, Lage, Germany). The animals were randomly distributed to the two study groups. All animal procedures were performed according to the National Institutes of Health guidelines for the use of experimental animals and the German legislation on the protection of animals and were approved by the local governmental animal welfare committee.

2.2. Diclofenac treatment

Thirty-three mice (male $n = 14$, female $n = 19$) were treated daily by an intraperitoneal (i.p.) injection of 5 mg/kg body weight (BW) diclofenac (Sigma-Aldrich, Taufkirchen, Germany), starting from the day of surgery. Another 29 mice (male $n = 13$, female $n = 16$), which were treated with vehicle (saline), served as controls. The dose of diclofenac chosen in the present study is identical to the dose used in previous preclinical reports (Beck et al., 2003; Krischak et al., 2007; Ramirez-Garcia-Luna et al., 2019; Spiro et al., 2010; Simon and O'Connor, 2007). Mice were sacrificed by an overdose of barbiturates and femora were harvested for further biomechanical, micro computed tomographic (μCT) and histological analyses at 2 weeks (control: $n = 12$; diclofenac: $n = 15$) and 5 weeks (control: $n = 11$; diclofenac: n = 12) after fracture. Additionally, 12 mice ($n = 6$ each group) were sacrificed at 2 weeks after fracture for Western blot analyses of the callus tissue.

2.3. Surgical procedure

Mice were anesthetized by i.p. injection of ketamine (90 mg/kg BW, Ursotamin®, Serumwerke Bernburg, Bernburg, Germany) and xylazine (12 mg/kg BW, Rompun®, Bayer, Leverkusen, Germany). A medial parapatellar incision was performed under aseptic conditions at the right knee and the patella was dislocated laterally. After drilling a hole (diameter of 0.5 mm) into the intercondylar notch an injection needle with a diameter of 0.4 mm was placed into the intramedullary canal. Subsequently, a tungsten guidewire (diameter of 0.2 mm) was inserted through the needle. After removal of the needle, the femur was fractured by a 3-point bending device and an intramedullary medical stainless steel screw (length of 17.2 mm, diameter of 0.5 mm; AO Foundation, Research Implants System, Davos, Switzerland) was implanted over the guidewire to stabilize the fracture (Holstein et al., 2009). After fixation of the fracture, the wound was closed using 5–0 synthetic sutures. Adequate reduction of the fracture and position of the implant were confirmed by radiography (MX-20, Faxitron X-ray Corporation, Wheelin, IL, USA). All fractures were simple, transverse midshaft fractures according to the AO classification type A2 fracture. In none of the animals an incomplete fracture was observed. For analgesia the mice received tramadol-hydrochloride (Grünenthal, Aachen, Germany) in the drinking water (1 mg/mL) from day 1 before surgery until day 7 after surgery.

2.4. X-ray analysis

At the end of the observation period the animals were re-anesthetized and lateral X-rays (MX-20, Faxitron X-ray Corporation) of the healing femora were performed. Fracture healing was analyzed according to the classification of Goldberg with stage 0 indicating radiological nonunion, stage 1 indicating possible union and stage 2 indicating radiological union (Goldberg et al., 1985).

2.5. Biomechanical analysis

For biochemical analysis, femora were resected at 2 and 5 weeks after fracture and freed from soft tissue. After removal of the implants, callus stiffness was measured using a three-point bending device (Mini-Zwick Z 2.5; Zwick, Ulm, Germany). Due to the different time points of healing studied, the loads which had to be applied varied markedly between the individual animals. Loading was stopped individually in every case when the actual load-displacement curve deviated >1 % from linearity (Schoen et al., 2008). To guarantee standardized measuring conditions, femora were always mounted with the ventral aspect upwards. A working gauge length of 6 mm was used. Applying a gradually increasing bending force with 1 mm/min, the bending stiffness (N/mm) was calculated from the linear elastic part of the load displacement diagram. The loads applied ranged up to 3 N at 2 weeks and up to 18 N at 5 weeks after fracture in both study groups. The application of a non-destructive force was controlled macroscopically and, later on, microscopically during the histological analysis by Safranin-O staining. The tissue slides were analyzed on whether a re-fracture has occurred. Notably, we could not detect any signs of re-fracture in the Safranin-O histologies in both study groups. To account for differences in bone stiffness of the individual animals, the unfractured left femora were also analyzed, serving as internal control. Values of the fractured femora are given in percent of the corresponding unfractured femora.

2.6. μ-CT analysis

The specimens were scanned (Skyscan 1172, Bruker, Billerica, MA) at a spatial resolution of 6.5 μm with a standardized setup (tube voltage: 50 kV; current: 100 μA; intervals: 0.4°; exposure time: 3500 ms; filter: 0.5 mm aluminum). Images were stored in three-dimensional arrays. To express grey values as mineral content (bone mineral density; BMD), calcium hydroxyapatite (CaHA) phantom rods with known BMD values (0.250 g and 0.750 g CaHA/cm^3) were employed for calibration. The region of interest (ROI) defining the novel bone was contoured manually excluding any original cortical bone. The thresholding allowed the differentiation between low and highly mineralized bone. The thresholds to distinguish between poorly and highly mineralized bone were based upon visual inspection of the images, qualitative comparison with histological sections and other studies investigating bone repair and callus tissue by μCT (Bosemark et al., 2013; Morgan et al., 2009; Isaksson et al., 2009). A BMD with >0.642 g/cm^3, resulting in grey values of 98–255, was defined as highly mineralized bone. Poorly mineralized bone was defined to have a BMD value between 0.410 g/cm^3 and 0.642 g/cm^3resulting in grey values of 68–97.

The following parameters were calculated from the callus region of interest for each specimen: tissue volume (TV) (mm^3), total bone volume fraction of tissue volume (BV/TV (%), poorly mineralized bone volume fraction of TV (%), highly mineralized bone volume fraction of TV (%), trabecular thickness (mm), trabecular separation (mm) and trabecular number (1/mm).

2.7. Histomorphometric analysis

For histological analysis, femora were analyzed at 2 and 5 weeks after fracture healing. The bones were fixed in immunohistochemistry (IHC) zinc fixative (BD Pharmingen, San Diego, CA) for 24 h, decalcified in 13 % EDTA solution for 2 weeks and then embedded in paraffin. Longitudinal sections of 5 μm thickness were stained with Safranin-O. At a magnification of 12.5 × (BX60, Olympus, Tokyo, Japan; Axio Cam and Axio Vision 3.1, Carl Zeiss, Oberkochen, Germany) structural indices were calculated according to the suggestion provided by Gerstenfeld et al. (Gerstenfeld et al., 2005) using the ImageJ Analysis System (NIH, Bethesda, MD, USA). These included visible callus area (bone, cartilaginous and fibrous callus area)/femoral bone diameter (cortical width plus marrow diameter) at the fracture gap (CAr/BDm (mm)), callus tissue diameter/femora bone diameter at the fracture gap (CDm/BDm), bone (total osseous tissue) callus area/visible callus area (TOTAr/CAr (%)), cartilaginous callus area/visible callus area (CgAr/CAr (%)), and fibrous tissue callus area/visible callus area (FTAr/CAr (%)). In addition, we used a score system (histo-score) to evaluate the quality of fracture bridging (Garcia et al., 2008). Both cortices were analyzed for bone bridging (2 points), cartilage bridging (1 point) or bridging with fibrous tissue (0 point). This score system results in a maximum of 4 points for each specimen, indicating complete bone bridging. Notably Areas with no visible tissue within the callus were excluded from the measurement.

In addition, the morphology of novel bone tissue was analyzed by determining the ratio of the woven bone callus area/bone (total osseous tissue) callus area (WbAr/TOTAr (%)) and the ratio of lamellar bone callus area/bone (total osseous tissue) callus area (LmbAr/TOTAr (%)) at the fracture gap. For this purpose, one high power field (HPF; 200 × magnification) was placed in a standardized manner at the fracture gap of each of the two cortices. Afterwards the total area of bone tissue was measured within the HPF. Subsequently, the area of lamellar bone was measured, according to its typical morphology of structured parallel-running fibres (Shapiro and Wu, 2019). To calculate the area of woven bone, the ratio of lamellar bone was subtracted from the total area of bone tissue.

Moreover, tartrate-resistant acid phosphatase (TRAP) activity was analyzed in the callus at 2 and 5 weeks after fracture. For this purpose, bones were fixed in IHC zinc fixative for 24 h, decalcified in 13 % EDTA solution for 2 weeks and then embedded in paraffin. After deparaffinizing, longitudinal sections of 5 μm thickness were incubated in a mixture of 5 mg naphthol AS-MX phosphate and 11 mg fast red TR salt in 10 mL 0.2 M sodium acetate buffer (pH 5.0) for 1 h at 37 °C. Sections were counterstained with methyl green and covered with glycerine gelatine. TRAP-positive multinucleated cells (three or more nuclei per cell) were counted. In 2-week specimens five high-power fields (HPFs; 400 × magnification) were placed at each site within the periosteal region of the callus. Thus, a total of 10 HPFs were analyzed from each specimen. Because of the reduced size of the callus at 5 weeks, only 6 HPFs per specimen were studied. The data on histomorphological osteoclast analyses are given as numbers of osteoclasts per HPF.

2.8. Western blot analysis

Protein expression within the callus tissue was determined by Western blot analysis, including the expression of bone morphogenetic protein (BMP)-2 , cysteine-rich protein (CYR) 61, receptor activator of NF- κB ligand (RANKL), osteoprotegerin (OPG), collagen (col)-2 and col-10. Moreover, the RANKL/OPG-ratio was calculated for each individual animal and then averaged for each study group. The callus tissue was frozen and stored at −80 °C until required. Analyses were performed from callus tissue at 2 weeks after fracture healing ($n = 6$ each group). After saving the whole protein fraction, analysis was performed using the following antibodies: rabbit anti-mouse BMP-2 (1:100, Santa Cruz Biotechnology, Heidelberg, Germany), goat anti-mouse CYR 61 (1:100, Santa Cruz Biotechnology), rabbit anti-mouse RANKL (1:100, Abcam, Cambridge, UK), rabbit anti-mouse OPG (1:300, Biozol Diagnostica, Eching, Germany), rabbit anti-mouse col-2 (1:50, Biozol Diagnostica) and rabbit anti-mouse col-10 (1:50, Biozol Diagnostica). Primary antibodies were followed by corresponding horseradish peroxidase-conjugated secondary antibodies (1:1000, R&D Systems, Minneapolis, USA; DakoCytomation, Hamburg, Germany). Protein expression was visualized by means of luminol-enhanced chemiluminescence after exposure of the membrane to the Intas ECL Chemocam Imager (Intas Science Imaging Instrument GmbH, Göttingen, Germany) and normalized to β–actin signals (1:5000, mouse anti-mouse β-actin, Sigma-Aldrich) to correct for unequal loading.

2.9. Statistics

All data are given as means ± SEM. After proving the assumption for normal distribution (Kolmogorov-Smirnov test) and equal variance (F-test), comparisons between the two experimental groups were performed by a Student's *t*-test. For non-parametrical data, a Mann-Whitney *U* test was used. Moreover, a 3-way ANOVA, treatment × time × sex on the main outcome parameter "bending stiffness" was performed. The 3-way ANOVA was followed by the Holm-Sidak test. Statistics were performed using SigmaPlot 13.0 software (Systat Software GmbH, Erkrath, Germany). A p-value <0.05 was considered to indicate significant differences.

3. Results

3.1. X-ray analysis

The X-rays performed at 2 and 5 weeks after fracture confirmed a transverse midshaft femur fracture and the adequate positioning of the intramedullary screw in each animal (Fig. 1a and b). The radiological analysis revealed that the Goldberg score did not differ between the two study groups at 2 (1.0 ± 0.0 vs. 1.0 ± 0.0) and 5 weeks (1.67 ± 0.14 vs.1.91 ± 0.09) after fracture.

3.2. Biomechanical analysis

At 2 weeks after fracture the biomechanical analysis showed no significant difference in the relative bending stiffness between controls and diclofenac-treated animals (Fig. 1c). At 5 weeks after fracture, however, the analysis revealed a significantly lower relative bending stiffness in diclofenac-treated animals when compared to controls (Fig. 1d). In line with these results the absolute values of the bending stiffness at 2 weeks showed also no significant difference between controls (3.3 ± 0.5 N/mm) and diclofenac-treated animals (4.6 ± 0.6 N/mm; $p > 0.05$). Furthermore, at 5 weeks the analysis demonstrated significantly lower absolute bending stiffness values in diclofenac-treated animals (24.8 ± 4.0 N/mm) when compared to controls (53.6 ± 9.8 N/mm; $p < 0.05$). The additional analysis with the 3-way ANOVA demonstrated that treatment and time, but not sex, had a significant effect on the main outcome parameter bending stiffness.

Of note, we found no significant difference in the bending stiffness of the contralateral, non-fractured femora at 2 weeks (control: 103.0 ± 5.1 N/mm vs. diclofenac: 106.8 ± 8.3 N/mm; $p > 0.05$) and 5 weeks (control: 105.4 ± 6.3 N/mm vs. diclofenac: 98.3 vs. 4.8 N/mm; $p > 0.05$) after fracture.

3.3. μCT analysis

The μCT analysis revealed a typical pattern of secondary fracture healing in controls and diclofenac-treated animals at 2 and 5 weeks after fracture. This was indicated by the formation of a large fracture callus at 2 weeks after fracture and the subsequent bony bridging and remodeling at 5 weeks after fracture (Fig. 1e and f). The analysis showed that the

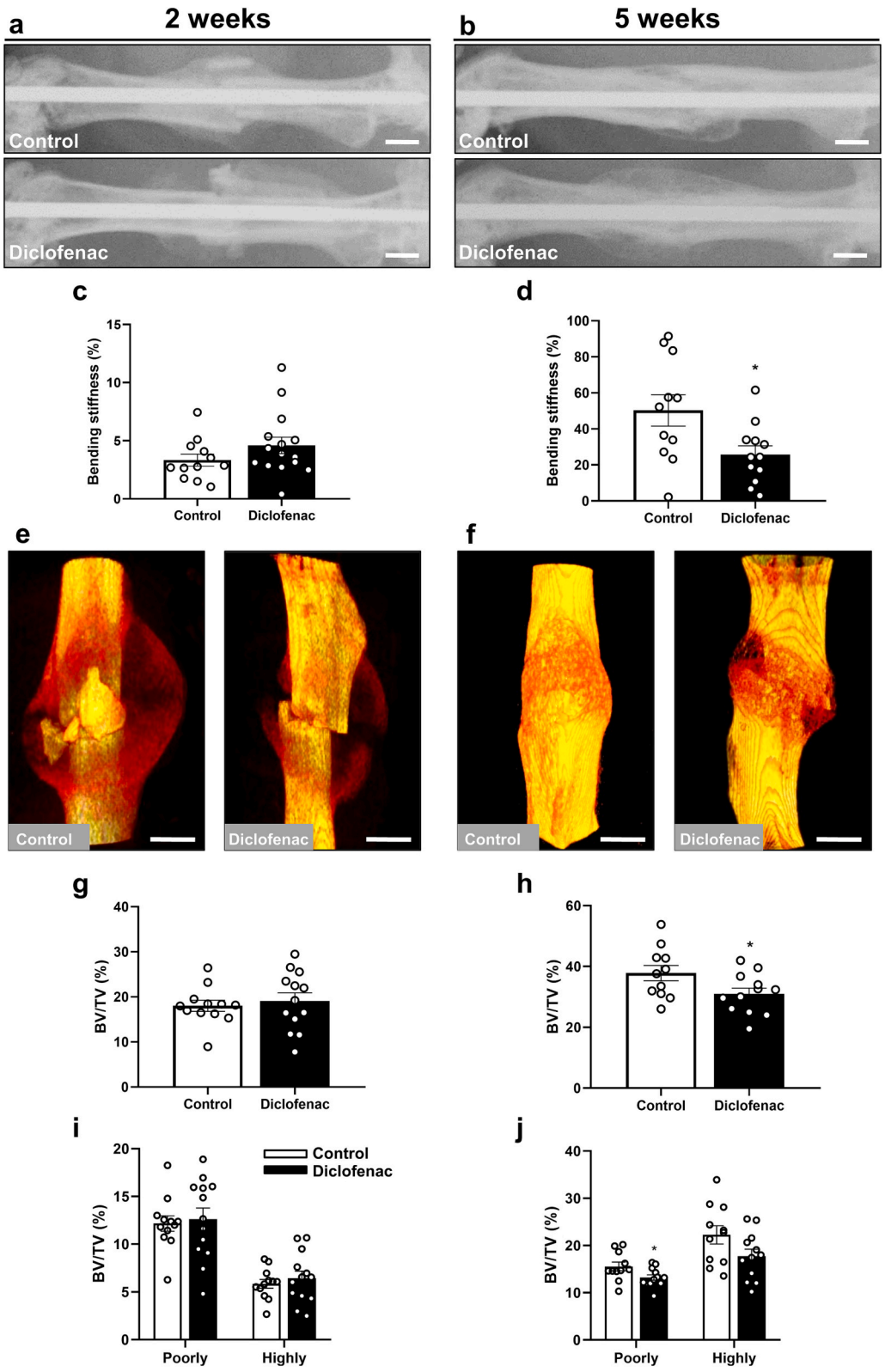

Fig. 1. Representative X-rays of fractured mouse femora stabilized by an intramedullary screw in controls and diclofenac-treated animals at 2 (**a**) and 5 weeks (**b**) after fracture. Scale bars: 1 mm. Biomechanical analysis of bending stiffness in controls (*white bars*) and diclofenac-treated animals (*black bars*) at 2 (**c**) and 5 weeks (**d**) after fracture. Data are given in percent to the contralateral, non-fractured femora (%). Representative μCT images of mouse femora in controls and diclofenac-treated animals at 2 (**e**) and 5 weeks (**f**) after fracture. μCT analysis of bone volume fraction of tissue volume (BV/TV (%) (**g**, **h**) and the poorly and highly mineralized bone fraction (%) (**i**, **j**) in controls (*white bars*) and diclofenac-treated animals (*black bars*) at 2 (**g**, **i**) and 5 weeks (**h**, **j**) after fracture. Means ± SEM; $n = 11–15$; *$p <$ 0.05 vs. control.

BV/TV was not affected at 2 weeks after fracture in diclofenac-treated animals (Fig. 1g). However, at 5 weeks after fracture the μCT analysis revealed a significantly reduced BV/TV in diclofenac-treated animals when compared to controls (Fig. 1h). In addition, our results demonstrated that the fraction of poorly and highly mineralized bone tissue showed no significant differences between the two study groups at 2 weeks after surgery (Fig. 1i), whereas at 5 weeks the data revealed a significantly reduced fraction of poorly mineralized bone tissue (Fig. 1j).

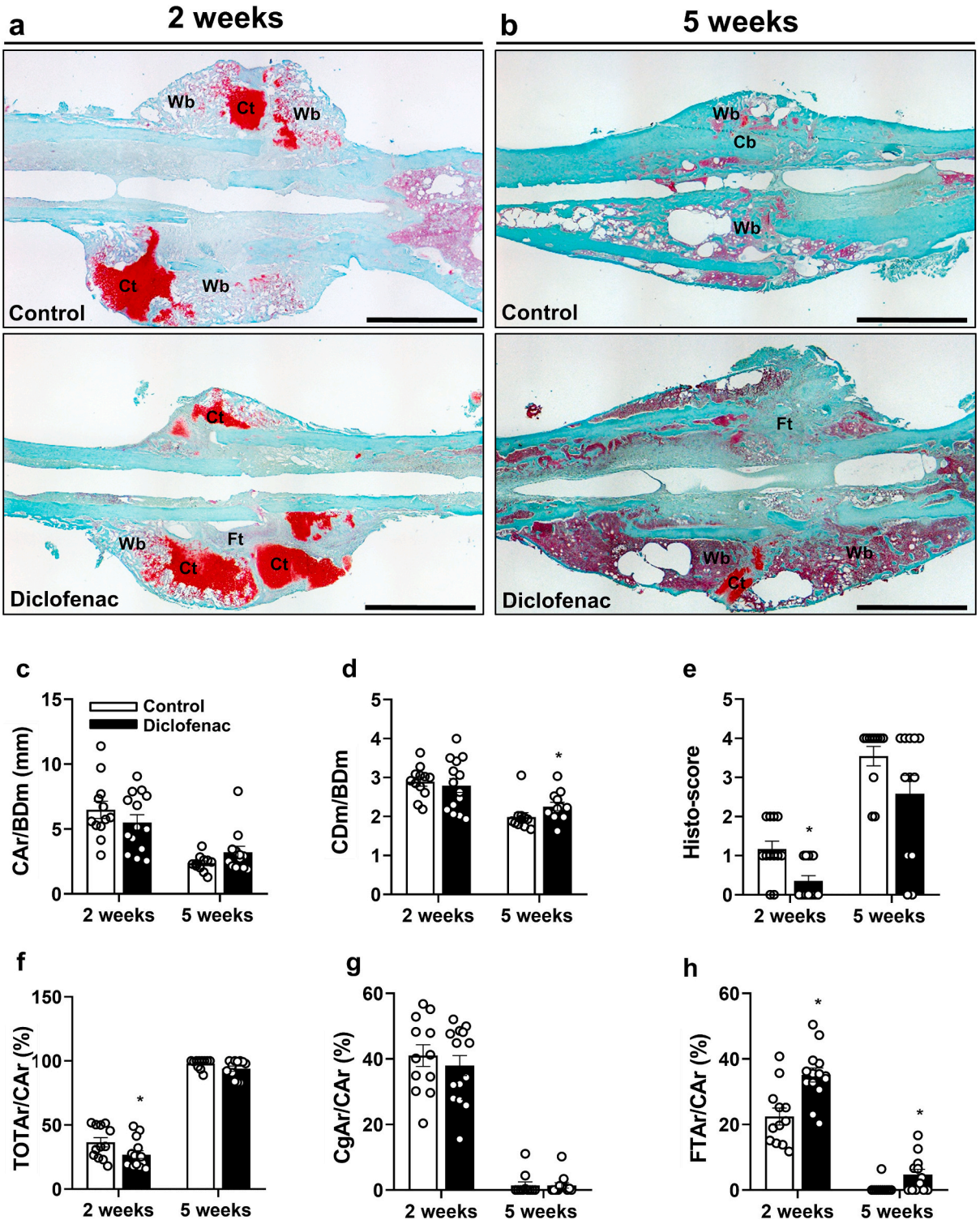

Fig. 2. Representative histological images of Safranin-O-stained femora of controls and diclofenac-treated animals at 2 (**a**) and 5 weeks (**b**) after fracture. Fibrous tissue (Ft), cartilaginous tissue (Ct), woven bone (Wb) and cortical bone (Cb) are indicated. Scale bars: 2 mm. Histomorphometric analysis of visible callus area (bone, cartilaginous and fibrous callus area)/femoral bone diameter (cortical width plus marrow diameter) at the fracture gap (CAr/BDm (mm)) (**c**), callus tissue diameter/femoral bone diameter at the fracture gap (CDm/BDm) (**d**), histo-score (**e**), bone (total osseous tissue) callus area/visible callus area (TOTAr/CAr (%)) (**f**), cartilaginous callus area/visible callus area (CgAr/CAr (%)) (**g**) and fibrous tissue callus area/visible callus area (FTAr/CAr (%)) (**h**) in controls (*white bars*) and diclofenac-treated animals (*black bars*) at 2 and 5 weeks after fracture. Means ± SEM; $n = 11–15$; *$p < 0.05$ vs. control.

Further analyses of the trabecular architecture, including trabecular thickness, number and separation revealed no significant difference between the two study groups (Table 1 suppl).

3.4. Histomorphometric analysis

In line with the radiological analysis, the histomorphometric analysis revealed a typical pattern of secondary endochondral fracture healing in both study groups at 2 and 5 weeks after fracture (Fig. 2a and b). The relation of callus area to femoral diameter was not significantly affected by diclofenac treatment (Fig. 2c). At 5 weeks after fracture, the analysis showed a significantly larger callus diameter in relation to the femoral diameter (CDm/BDm) in diclofenac-treated mice, when compared to controls (Fig. 2d). At 2 weeks after fracture, the callus diameter was not significantly affected by diclofenac treatment (Fig. 2d). The histomorphometric analysis showed further a significantly reduced Histoscore at 2 weeks after fracture in diclofenac-treated animals (Fig. 2e). The analyses of the composition of the callus tissue revealed a significantly reduced amount of bone tissue at 2 weeks after fracture in the diclofenac group (Fig. 2f). The amount of cartilage tissue was not different in diclofenac-treated animals when compared to controls (Fig. 2g). Of note, the amount of fibrous tissue was significantly higher at 2 and 5 weeks after fracture in diclofenac-treated animals, when compared to controls. (Fig. 2h).

At 2 weeks after fracture the analysis of the morphology of newly formed bone tissue did not show any significant difference between the two study groups (Fig. 3a–f). However, at 5 weeks after fracture the newly formed bone tissue at the fracture site revealed a significantly reduced amount of lamellar bone and a significantly enhanced amount of woven bone in diclofenac-treated animals when compared to controls (Fig. 3a–f).

Additional histological analyses of the number of TRAP-positive osteoclasts within the callus tissue of fractured femora showed a significantly reduced number of TRAP-positive osteoclasts at 2 weeks after fracture in diclofenac-treated mice (Fig. 3g and h). In contrast, 5 weeks of diclofenac treatment resulted in a significantly increased number of TRAP-positive osteoclasts when compared to controls (Fig. 3g and h).

3.5. Western blot analysis

At 2 weeks after fracture the Western blot analysis of the callus tissue demonstrated no difference in the expression of RANKL, a stimulator of osteoclastogenesis (Boyce and Xing, 2008), between the two study groups. However, the expression of OPG, an inhibitor of osteoclastogenesis (Boyce and Xing, 2008), was significantly enhanced in diclofenac-treated animals (Fig. 4a–c). The RANKL/OPG-ratio was not significantly affected in diclofenac-treated aged mice (Fig. 4d). The expression of the bone formation marker BMP-2 and the pro-angiogenic factor CYR61 after 2 weeks of diclofenac treatment demonstrated no significant difference when compared to controls (Fig. 4e–g). The expression of col-2, a marker of chondrocytes in early callus formation (Sandberg et al., 1993), was significantly increased in diclofenac-treated animals, whereas the expression col-10, a marker for hypertrophic chondrocytes (Grant et al., 1987), did not significantly differ when compared to controls (Fig. 4h–j).

4. Discussion

The aim of the present study was to analyze the effect of diclofenac treatment on fracture healing in aged mice. Our findings suggest that diclofenac delays callus remodeling and bone healing, as indicated by a reduced bone formation and a lower amount of lamellar bone within the callus tissue, resulting in a decreased bending stiffness of the fractured femora. Interestingly, the impaired fracture repair was associated with an affected number and activity of osteoclasts within the callus tissue.

Despite growing evidence of their detrimental effects on fracture healing, NSAIDs remain among the most common analgesic medications after trauma and surgical interventions, also among older patients (Zhou et al., 2014; Moore and Scheiman, 2018). A variety of preclinical studies demonstrated that diclofenac has negative effects on the process of bone regeneration. Beck et al. (Beck et al., 2003) demonstrated in a tibia-osteotomy model in Wistar rats that diclofenac short-term (7 days) and long-term (21 days) treatment results in a significantly reduced breaking force, bending stiffness and bone density. Using the same osteotomy model, Krischak et al. (Krischak et al., 2007) showed that diclofenac long-term treatment leads to a delayed callus maturation and endochondral ossification indicated by higher amounts of cartilage within the callus tissue. In another study, Spiro et al. (Spiro et al., 2010) investigated the effect of diclofenac treatment of fracture healing and BMP-7 induced ectopic bone formation in 12-week-old C57BL/6-mice. The authors found a reduced BV/TV % within the callus tissue and a decreased force to failure in fractured femora at 20 after surgery as well as a lower BV/TV % within the ectopic bone nodule of diclofenac-treated mice. Moreover, Ramirez-Garcia-Luna et al. (Ramirez-Garcia-Luna et al., 2019) found a significantly reduced bone volume in a bilateral femoral defect mouse in diclofenac-treated mice 2 weeks after surgery. Additionally in a recent study, Lehmann et al. (Lehmann et al., 2021) found a significantly reduced trabecular bone volume and mineral density after 30 days of diclofenac treatment in 9-week-old C57BL/6-mice. These findings are in line with our results, as we demonstrated a reduced bone volume and increased amount of fibrous tissue within the callus of diclofenac-treated animals at 2 weeks after surgery. Moreover, our analysis revealed a decreased bending stiffness and BV/TV % at 5 weeks after fracture. Notably, however, we did not detect a reduced bending stiffness at the early 2 weeks observation time point. Taken together, the analysis suggests that diclofenac-treatment in aged animals has similar detrimental effects on bone regeneration when compared to studies investigating the effects in young adult animals. However, the negative effects on fracture healing by diclofenac may be delayed in aged animals.

After oral uptake Diclofenac will be completely resorbed by the gastrointestinal tract (Davies and Anderson, 1997). Approximately 60 % of the drug reaches the systemic circulation due to a first-pass effect of the liver (Davies and Anderson, 1997). The blood plasma Diclofenac is >99 % bound in plasma to proteins, primarily to albumin (Riess et al., 1978). In inflamed tissue, the weakly acidic environment prevailing there reduces protein binding. The resulting free diclofenac can diffuse more easily into intracellular spaces and exert its effect there (Altman et al., 2015). The plasma half-life of diclofenac in mice is approximately 30 min (Wilson et al., 2018). The drug is metabolized in the liver and subsequently excreted biliarily and renally (Small, 1989). Sarda et al. (2012) investigated the diclofenac metabolism in mice by high performance liquid chromatography. The authors detected major routes of metabolism, which included a conjugation with taurine; and hydroxylation (probably at the 4′-and 5-arene positions) followed by conjugation to taurine, glucuronic acid or glucose. Notably, the detected mechanisms involved in the generation of benzoic acid and indolinone products indicated the formation of reactive intermediates in vivo that may possibly contribute to hepatotoxicity.

NSAIDs like diclofenac inhibit COX-2, which is expressed in response to bone injury and is necessary for the synthesis of prostaglandin E2 (Simon and O'Connor, 2007). The release of prostaglandin E2 is crucial for the upregulation of RANKL and the inhibition of OPG in osteoblasts, resulting in an accumulation of osteoclasts in the early phase of fracture healing (Blackwell et al., 2010). Notably, osteoclasts play a vital role in the process of bone regeneration and remodeling by osteoclast-mediated cartilage and bone resorption (Schindeler et al., 2008). Moreover, their inhibition is associated with a delayed fracture healing (Soung do et al., 2013). In line with these findings our biomechanical, radiographic and histological data show a reduced bone formation and bending stiffness as well a larger callus size after diclofenac treatment. This was associated with a significantly lower number of TRAP-positive osteoclasts at 2

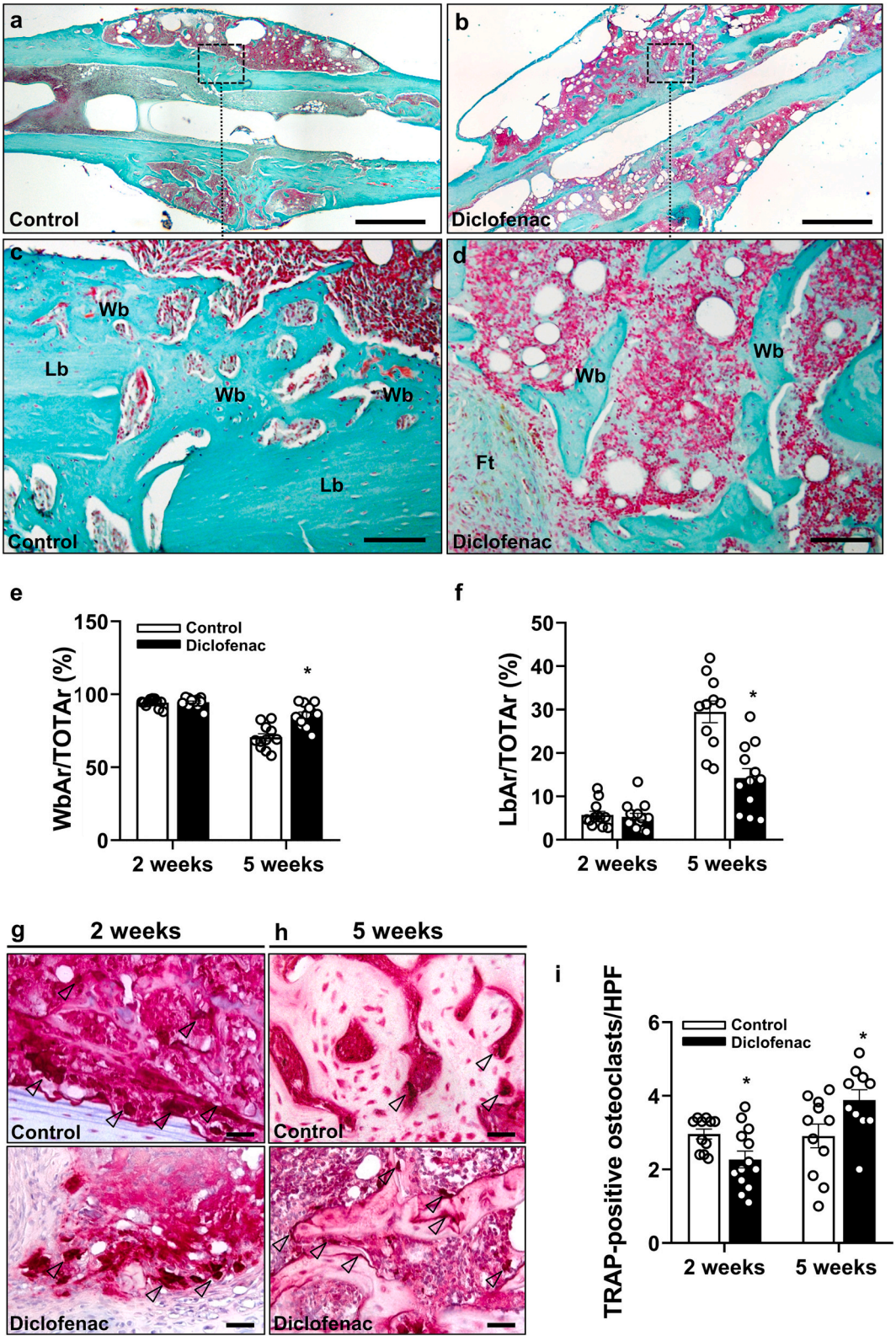

Fig. 3. Representative histological images of the Safranin-O-stained mouse femora of a control (**a**) and a diclofenac-treated animal (**b**) at 5 weeks after fracture. Scale bars: 1 mm. Higher magnification of the inserts in a and b, demonstrating callus tissue at the fracture gap in the control (**c**) and the diclofenac-treated (**d**) animal. Fibrous tissue (Ft), woven bone (Wb) and lamellar bone (Lb) are indicated. Scale bars: 100 μm. Histomorphometric analysis of the ratio of the woven bone callus area/bone (total osseous tissue) callus area (WbAr/TOTAr (%)) (**e**) and the ratio of lamellar bone callus area/bone (total osseous tissue) callus area (LmbAr/TOTAr (%)) (**f**) at the fracture gap in controls (*white bars*) and diclofenac-treated animals (*black bars*) at 2 and 5 weeks after fracture. Representative histological images of Safranin-O-stained femora of controls and diclofenac-treated animals at 2 (**g**) and 5 weeks (**h**) after fracture. Scale bar: 50 μm. Quantitative analysis (**i**) of the number of TRAP-positive osteoclasts per HPF within the callus tissue of controls (*white bars*) and diclofenac-treated animals (*black bars*) at 2 and 5 weeks after fracture. Means ± SEM; n = 11–15; *$p < 0.05$ vs. control.

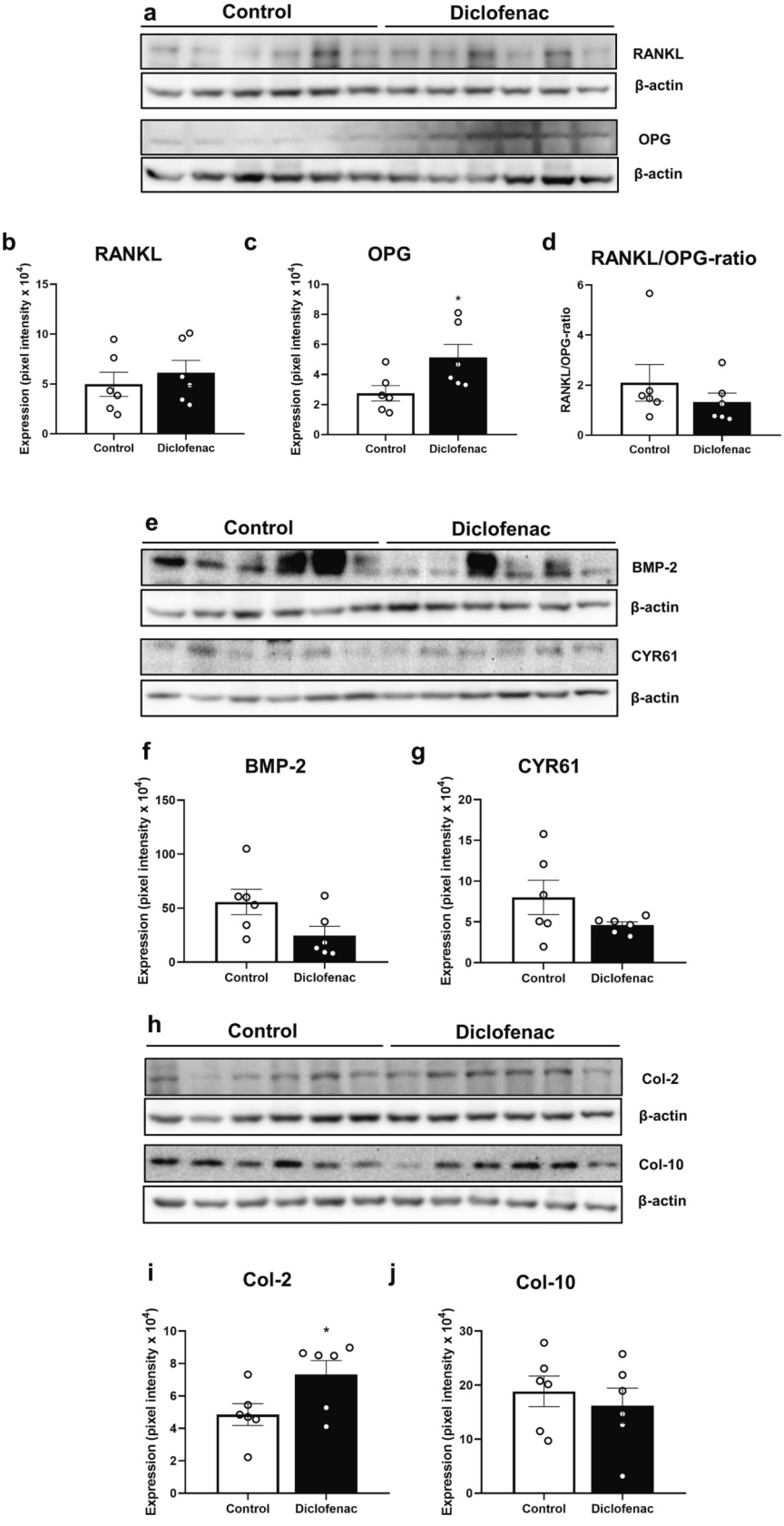

Fig. 4. Western blot analysis of the expression of RANKL (**a**, **b**), OPG (**a**, **c**) and RANKL/OPG-ratio (**d**) within the callus tissue of controls (*white bars*) and diclofenac-treated animals (*black bars*) at 2 weeks after fracture. Western blot analysis of the expression of BMP-2 (**e**, **f**) and CYR61 (**e**, **g**) within the callus tissue of controls (*white bars*) and diclofenac-treated animals (*black bars*) at 2 weeks after fracture. Western blot analysis of the expression of col-2 (**h**, **i**) and col-10 (**h**, **j**) within the callus tissue of controls (*white bars*) and diclofenac-treated animals (*black bars*) at 2 weeks after fracture. Means ± SEM; $n = 6$; $^{*}p < 0.05$ vs. control.

weeks after fracture and a significantly enhanced expression of OPG within the callus tissue of diclofenac-treated aged animals. In contrast after 5 weeks of diclofenac treatment, we found a higher number of osteoclasts within the callus tissue. Hence, the impaired fracture healing observed in the present study may be due to the fact that diclofenac delayed osteoclast activation by affecting RANKL/RANK/OPG signaling. This view is further supported by our Western blot analysis of col-2 expression. In diclofenac-treated animals we found a significantly higher expression of col-2, which is typically expressed in the early phase of bone healing (Sandberg et al., 1993) indicating a delay in the process of regeneration. Moreover, our histological analysis demonstrated a significantly reduced amount of lamellar bone within the callus tissue of diclofenac-treated aged mice, indicating not only an impaired fracture healing but also a delay in callus remodeling.

BMP-2 is a member of the transforming growth factor-β superfamily and plays a crucial role in the signaling cascade in human fracture callus (Huang et al., 2008; Tsuji et al., 2006). BMP-2 acts during the early phase of bone formation by promoting differentiation of mesenchymal stem cells and osteoprogenitor cells into osteoblasts (Mi et al., 2013). BMP-2 expression is significantly reduced within the callus tissue of nonunions when compared to that of successfully healed fractures (Kwong et al., 2009). A number of preclinical in vitro and in vivo studies demonstrated the stimulating function of BMP-2 on osteogenesis through various paracrine and autocrine mechanisms (Huang et al., 2008; Tsuji et al., 2006; Mi et al., 2013; Cheng et al., 2003). Notably, BMP-2 expression is mediated by the COX-2-induced synthesis of prostaglandin E2 and its binding to the EP4 receptor on osteoclasts and osteoblasts (Arikawa et al., 2004). On the other hand, Li et al. (Li et al., 2014) demonstrated in an in vitro study using primary costosternal chondrocytes that BMP-2 can also directly induce COX-2 expression by a Smad-signaling pathway. However, in the present study we found no significant difference in the BMP-2 expression of diclofenac-treated mice and controls. These findings indicate that the impaired fracture healing in diclofenac-treated animals is not caused by a reduction in BMP-2 expression.

In conclusion, the present study demonstrates that diclofenac treatment impairs fracture healing in aged mice by affecting RANKL/RANK/OPG-mediated osteoclast formation. Therefore, diclofenac should be used with caution in geriatric patients after orthopedic trauma, particularly in cases with high risk of compromised fracture healing and nonunion formation.

Supplementary data to this article can be found online at https://doi.org/10.1016/j.exger.2023.112201.

CRediT authorship contribution statement

M.M.M.: data analysis, figure preparation, data discussion and interpretation, manuscript writing. M.S.: surgery, radiological, biomechanical and histological analysis. C.S.: Western blot analysis. B.J.B., M. F.R., S.C.H., S.E., A.N.: data discussion and interpretation, critical manuscript revision. M.W.L., M.D.M.: idea and study design, data interpretation, manuscript writing. T.H.: idea and study design, data discussion and interpretation, critical manuscript revision. All authors reviewed and approved the final version of the manuscript.

Declaration of competing interest

The authors declare that they have no conflict of interest.

Acknowledgements

We are grateful for the excellent technical assistance of Janine Becker and Julia Parakenings.

References

Altman, R., Bosch, B., Brune, K., et al., 2015. Advances in NSAID development: evolution of diclofenac products using pharmaceutical technology. Drugs 75, 859–877.
Arikawa, T., Omura, K., Morita, I., 2004. Regulation of bone morphogenetic protein-2 expression by endogenous prostaglandin E2 in human mesenchymal stem cells. J. Cell. Physiol. 200, 400–406.
Beck, A., Krischak, G., Sorg, T., et al., 2003. Influence of diclofenac (group of nonsteroidal anti-inflammatory drugs) on fracture healing. Arch. Orthop. Trauma Surg. 123, 327–332.
Blackwell, K.A., Raisz, L.G., Pilbeam, C.C., 2010. Prostaglandins in bone: bad cop, good cop? Trends Endocrinol. Metab. 21, 294–301.
Bosemark, P., Isaksson, H., McDonald, M.M., et al., 2013. Augmentation of autologous bone graft by a combination of bone morphogenic protein and bisphosphonate increased both callus volume and strength. Acta Orthop. 84, 106–111.
Boyce, B.F., Xing, L., 2008. Functions of RANKL/RANK/OPG in bone modeling and remodeling. Arch. Biochem. Biophys. 473, 139–146.
Cauley, J.A., Thompson, D.E., Ensrud, K.C., et al., 2000. Risk of mortality following clinical fractures. Osteoporos. Int. 11, 556–561.
Cheng, H., Jiang, W., Phillips, F.M., et al., 2003. Osteogenic activity of the fourteen types of human bone morphogenetic proteins (BMPs). J. Bone Joint Surg. Am. 85-A, 1544–1552.
Davies, N.M., Anderson, K.E., 1997. Clinical pharmacokinetics of diclofenac. Therapeutic insights and pitfalls. Clin. Pharmacokinet. 33, 184–213.
Dodwell, E.R., Latorre, J.G., Parisini, E., et al., 2010. NSAID exposure and risk of nonunion: a meta-analysis of case-control and cohort studies. Calcif. Tissue Int. 87, 193–202.
Garcia, P., Holstein, J.H., Histing, T., et al., 2008. A new technique for internal fixation of femoral fractures in mice: impact of stability on fracture healing. J. Biomech. 41, 1689–1696.
Gerstenfeld, L.C., Wronski, T.J., Hollinger, J.O., et al., 2005. Application of histomorphometric methods to the study of bone repair. J. Bone Miner. Res. 20, 1715–1722.
Goldberg, V.M., Powell, A., Shaffer, J.W., et al., 1985. Bone grafting: role of histocompatibility in transplantation. J. Orthop. Res. 3, 389–404.
Grant, W.T., Wang, G.J., Balian, G., 1987. Type X collagen synthesis during endochondral ossification in fracture repair. J. Biol. Chem. 262, 9844–9849.
Green, E., Lubahn, J.D., Evans, J., 2005. Risk factors, treatment, and outcomes associated with nonunion of the midshaft humerus fracture. J. Surg. Orthop. Adv. 14, 64–72.
Gruber, R., Koch, H., Doll, B.A., et al., 2006. Fracture healing in the elderly patient. Exp. Gerontol. 41, 1080–1093.
Haversath, M., Catelas, I., Li, X., et al., 2012. PGE(2) and BMP-2 in bone and cartilage metabolism: 2 intertwining pathways. Can. J. Physiol. Pharmacol. 90, 1434–1445.
Holstein, J.H., Matthys, R., Histing, T., et al., 2009. Development of a stable closed femoral fracture model in mice. J. Surg. Res. 153, 71–75.
Huang, Y.H., Polimeni, G., Qahash, M., 2008. Bone morphogenetic proteins and osseointegration: current knowledge - future possibilities. Periodontol 2000 (47), 206–223.
Isaksson, H., Grongroft, I., Wilson, W., et al., 2009. Remodeling of fracture callus in mice is consistent with mechanical loading and bone remodeling theory. J. Orthop. Res. 27, 664–672.
Klotz, U., 2009. Pharmacokinetics and drug metabolism in the elderly. Drug Metab. Rev. 41, 67–76.
Krischak, G.D., Augat, P., Sorg, T., et al., 2007. Effects of diclofenac on periosteal callus maturation in osteotomy healing in an animal model. Arch. Orthop. Trauma Surg. 127, 3–9.
Kwong, F.N., Hoyland, J.A., Evans, C.H., et al., 2009. Regional and cellular localisation of BMPs and their inhibitors' expression in human fractures. Int. Orthop. 33, 281–288.
Lehmann, T.P., Wojtkow, M., Pruszynska-Oszmalek, E., et al., 2021. Trabecular bone remodelling in the femur of C57BL/6J mice treated with diclofenac in combination with treadmill exercise. Acta Bioeng. Biomech. 23, 3–11.
Li, T.F., Yukata, K., Yin, G., et al., 2014. BMP-2 induces ATF4 phosphorylation in chondrocytes through a COX-2/PGE2 dependent signaling pathway. Osteoarthr. Cartil. 22, 481–489.
Lu, C., Miclau, T., Hu, D., et al., 2005. Cellular basis for age-related changes in fracture repair. J. Orthop. Res. 23, 1300–1307.
Mi, M., Jin, H., Wang, B., et al., 2013. Chondrocyte BMP2 signaling plays an essential role in bone fracture healing. Gene 512, 211–218.
Moore, N., Scheiman, J.M., 2018. Gastrointestinal safety and tolerability of oral non-aspirin over-the-counter analgesics. Postgrad. Med. 130, 188–199.
Morgan, E.F., Mason, Z.D., Chien, K.B., et al., 2009. Micro-computed tomography assessment of fracture healing: relationships among callus structure, composition, and mechanical function. Bone 44, 335–344.
Ramirez-Garcia-Luna, J.L., Wong, T.H., Chan, D., et al., 2019. Defective bone repair in diclofenac treated C57Bl6 mice with and without lipopolysaccharide induced systemic inflammation. J. Cell. Physiol. 234, 3078–3087.
Riess, W., Stierlin, H., Degen, P., et al., 1978. Pharmacokinetics and metabolism of the anti-inflammatory agent voltaren. Scand. J. Rheumatol. Suppl. 17–29.
Rollmann, M.F., Herath, S.C., Braun, B.J., et al., 2019. In-hospital mortality of pelvic ring fractures in older adults now and then: a pelvic registry study. Geriatr Gerontol Int 19, 24–29.
Rose, S., Maffulli, N., 1999. Hip fractures. An epidemiological review. Bull. Hosp. Jt Dis. 58, 197–201.
Sandberg, M.M., Aro, H.T., Vuorio, E.I., 1993. Gene expression during bone repair. Clin. Orthop. Relat. Res. 292–312.

Sarda, S., Page, C., Pickup, K., et al., 2012. Diclofenac metabolism in the mouse: novel in vivo metabolites identified by high performance liquid chromatography coupled to linear ion trap mass spectrometry. Xenobiotica 42, 179–194.
Schindeler, A., McDonald, M.M., Bokko, P., et al., 2008. Bone remodeling during fracture repair: the cellular picture. Semin. Cell Dev. Biol. 19, 459–466.
Schoen, M., Rotter, R., Schattner, S., et al., 2008. Introduction of a new interlocked intramedullary nailing device for stabilization of critically sized femoral defects in the rat: a combined biomechanical and animal experimental study. J. Orthop. Res. 26, 184–189.
Shapiro, F., Wu, J.Y., 2019. Woven bone overview: structural classification based on its integral role in developmental, repair and pathological bone formation throughout vertebrate groups. Eur. Cell. Mater. 38, 137–167.
Simon, A.M., O'Connor, J.P., 2007. Dose and time-dependent effects of cyclooxygenase-2 inhibition on fracture-healing. J. Bone Joint Surg. Am. 89, 500–511.
Small, R.E., 1989. Diclofenac sodium. Clin. Pharm. 8, 545–558.
Soung do, Y., Gentile, M.A., Duong, L.T., 2013. Effects of pharmacological inhibition of cathepsin K on fracture repair in mice. Bone 55, 248–255.
Spiro, A.S., Beil, F.T., Baranowsky, A., et al., 2010. BMP-7-induced ectopic bone formation and fracture healing is impaired by systemic NSAID application in C57BL/6-mice. J. Orthop. Res. 28, 785–791.
Tsuji, K., Bandyopadhyay, A., Harfe, B.D., et al., 2006. BMP2 activity, although dispensable for bone formation, is required for the initiation of fracture healing. Nat. Genet. 38, 1424–1429.
Wilson, C.E., Dickie, A.P., Schreiter, K., et al., 2018. The pharmacokinetics and metabolism of diclofenac in chimeric humanized and murinized FRG mice. Arch. Toxicol. 92, 1953–1967.
Zhou, Y., Boudreau, D.M., Freedman, A.N., 2014. Trends in the use of aspirin and nonsteroidal anti-inflammatory drugs in the general U.S. Population. Pharmacoepidemiol. Drug Saf. 23, 43–50.